Hydrodynamic fluctuations in the Kolmogorov flow: Nonlinear regime

I. Bena,[1] F. Baras,[2] and M. Malek Mansour[2]
[1]*Limburgs Universitair Centrum, B-3590 Diepenbeek, Belgium*
[2]*Centre for Nonlinear Phenomena and Complex Systems, Université Libre de Bruxelles, Campus Plaine, Code Postal 231, B-1050 Brussels, Belgium*
(Received 19 June 2000)

In a previous paper [I. Bena, M. Malek Mansour, and F. Baras, Phys. Rev. E **59**, 5503 (1999)] the statistical properties of linearized Kolmogorov flow were studied, using the formalism of fluctuating hydrodynamics. In this paper the nonlinear regime is considered, with emphasis on the statistical properties of the flow near the first instability. The normal form amplitude equation is derived for the case of an incompressible fluid and the velocity field is constructed explicitly above (but close to) the instability. The relative simplicity of this flow allows one to analyze the compressible case as well. Using a perturbative technique, it is shown that close to the instability threshold the stochastic dynamics of the system is governed by two coupled nonlinear Langevin equations in Fourier space. The solution of these equations can be cast into the exponential of a Landau-Ginzburg functional, which proves to be identical to the one obtained for the case of an incompressible fluid. The theoretical predictions are confirmed by numerical simulations of the nonlinear fluctuating hydrodynamic equations.

PACS number(s): 47.20.−k, 05.40.−a, 05.90.+m

I. INTRODUCTION

A central issue in nonequilibrium statistical physics is the role of fluctuations in the onset of hydrodynamic instabilities. From a theoretical point of view one generally relies on the Landau-Lifshitz fluctuating hydrodynamics [2], mainly because of its relative simplicity as compared to more fundamental approaches [3,4]. Fluctuating hydrodynamics has been used by various authors to study the statistical properties of simple fluids subjected to nonequilibrium constraints, such as temperature gradient [3,5,6] or shear [4,7] (for a review, see Ref. [8]). Light scattering results, obtained for systems under a temperature gradient, have shown quantitative agreement with theoretical predictions [9]. Quantitative agreement has also been demonstrated with results based on particle simulations, both for systems under temperature gradient [10,11] and shear [12].

Ordinarily the macroscopic study of subsonic hydrodynamic instabilities is based on the incompressibility assumption. However, as first pointed out by Zaitsev and Shliomis [13], this assumption is essentially inconsistent with the very foundations of the fluctuating hydrodynamics formalism since it imposes fictitious correlations between the velocity components of the fluid. On the other hand, the compressibility of the fluid affects mostly fast sound modes, whereas the dynamics of the system near an instability is governed by slow dissipative modes. We may thus expect that the behavior of a fluid evolving near a subsonic instability threshold is not affected in practice by its compressibility. This intuitive argument has been used by many authors who have considered fluctuating incompressible hydrodynamic equations, or even directly the corresponding normal form amplitude equations to which they added random noise terms [14]. In these approaches, the characteristics of the noise terms cannot be related to equilibrium statistical properties of the fluid and thus remain arbitrary. A more satisfactory approach would be to start with the full compressible fluctuating hydrodynamic equations. Reducing these equations to a final normal form amplitude equation near the instability would lead directly to the explicit form of the associated noise terms consistent with such requirements as the fluctuation-dissipation theorem. Such a procedure, however, proves to be quite difficult, mainly because of the boundary conditions. To our knowledge, the only attempt in this direction was made by Schmitz and Cohen for the case of the Bénard instability [15]. Concentrating on the behavior of a small layer in the bulk, these authors succeeded in deriving the linearized fluctuating equations close to the convective instability. Whether this technique can be generalized to derive the corresponding normal form amplitude equation for the case of the Bénard instability is not clear at the present time.

Recently, we have considered the problem of hydrodynamic fluctuations in the case of a simple flow proposed some 50 years ago by Kolmogorov [16]. Thanks to the periodic boundary conditions associated with this model, a detailed analysis of the linearized fluctuating hydrodynamic equations, from near equilibrium up to the vicinity of the first instability, could be carried out [1]. In particular, we have been able to show that in the long time limit the flow behaves as if the fluid were incompressible, regardless of the value of the Reynolds number. The situation was different for the short time behavior. We established that the incompressibility assumption leads here to a wrong form of the static correlation functions, in agreement with the prediction of Zaitsev and Shliomis [13], except near the instability threshold, where our results strongly suggest that the incompressibility assumption becomes valid again. On the other hand, the linearized fluctuating hydrodynamic equations are clearly not valid close to or beyond the instability threshold. Although extensive numerical simulations have confirmed our predictions, a satisfactory answer to this important problem requires a full nonlinear analysis of the fluctuating Kolmogorov flow. The present article is devoted to this problem.

In the next section, the Kolmogorov flow is briefly reviewed. A nonlinear analysis is carried out for an incom-

pressible fluid and the explicit form of the stream function and the associated velocity field is derived above but close to the instability. Section III is devoted to the analysis of a compressible fluid. After setting up a perturbation scheme, we show that the solution of the problem is essentially the same as the one derived in Sec. II for the incompressible fluid, at least close to the instability threshold. We then concentrate on the statistical properties of the flow and show that, close to the instability threshold, the dynamics of the system is governed by a set of two nonlinear coupled Langevin equations. Here again, the equivalence with the incompressible case is established. Concluding remarks and perspectives are summarized in Sec. IV.

II. INCOMPRESSIBLE KOLMOGOROV FLOW

Consider an isothermal flow in a rectangular box $L_x \times L_y$ oriented along the main axes, that is, $\{0 \leqslant x \leqslant L_x, 0 \leqslant y \leqslant L_y\}$. Periodic boundary conditions are assumed in both directions and the flow is maintained through an external force field of the form

$$\mathbf{F}_{ext} = F_0 \sin(2\pi n y/L_y)\,\mathbf{1}_x, \tag{1}$$

where $\mathbf{1}_x$ is the unit vector in the x direction. This model represents the so-called *Kolmogorov flow* and it belongs to the wider class of two-dimensional negative eddy viscosity flows [17]. It is entirely characterized through the strength of the force field F_0, the parameter n, which controls the wave number of the forcing, and the aspect ratio a_r, defined as

$$a_r = L_x/L_y. \tag{2}$$

In the following, we will mainly concentrate on the case $n=1$.

The fluctuating hydrodynamic equations for this model read:

$$\frac{\partial \rho}{\partial t} = -\boldsymbol{\nabla}\cdot(\rho\,\mathbf{v}), \tag{3}$$

$$\rho\frac{\partial \mathbf{v}}{\partial t} = -\rho\,(\mathbf{v}\cdot\boldsymbol{\nabla})\,\mathbf{v} - \boldsymbol{\nabla} p - \boldsymbol{\nabla}\cdot\boldsymbol{\sigma} + \mathbf{F}_{ext}, \tag{4}$$

where ρ is the mass density, p the hydrostatic pressure and $\boldsymbol{\sigma}$ the *two dimensional* fluctuating stress tensor,

$$\sigma_{i,j} = -\eta\left(\frac{\partial v_i}{\partial x_j} + \frac{\partial v_j}{\partial x_i} - \delta_{i,j}\,\boldsymbol{\nabla}\cdot\mathbf{v}\right) - \zeta\,\delta_{i,j}\,\boldsymbol{\nabla}\cdot\mathbf{v} + S_{i,j}. \tag{5}$$

$\mathbf{S}$ is a random tensor whose elements $\{S_{i,j}\}$ are Gaussian white noises with zero mean and covariances given by

$$\langle S_{i,j}(\mathbf{r},t)\,S_{k,l}(\mathbf{r}',t')\rangle = 2k_BT_0\,\delta(t-t')\,\delta(\mathbf{r}-\mathbf{r}')[\,\eta(\delta^{Kr}_{i,k}\delta^{Kr}_{j,l} + \delta^{Kr}_{i,l}\delta^{Kr}_{j,k}) + (\zeta-\eta)\,\delta^{Kr}_{i,j}\delta^{Kr}_{k,l}]. \tag{6}$$

For simplicity, we shall assume that the shear and bulk viscosity coefficients η and ζ are *state independent*, i.e., they are constant.

Let us first concentrate on the *deterministic* behavior. It can easily be checked that in the stationary state the pressure and density are uniform in space ($p_{st}=p_0$, $\rho_{st}=\rho_0$), whereas the velocity profile is given by

$$\mathbf{v}_{st} = u_0 \sin(2\pi y/L_y)\,\mathbf{1}_x,$$

$$u_0 = \frac{F_0 L_y^2}{4\pi^2\,\eta}. \tag{7}$$

For small enough F_0, this stationary flow is stable. As we increase F_0, however, the flow eventually becomes unstable, giving rise to rotating convective patterns. Other instabilities of increasing complexity may occur for larger values of F_0, culminating in a chaoticlike behavior similar to what is observed in turbulent flows [18–20]. In this paper we shall limit ourselves to the analysis of the system near its first instability.

We still have to supply the momentum conservation equation (4) with an equation of state relating the pressure to the density (recall that the system is isothermal). In this section, we shall simply assume that the flow is incompressible, i.e.,

$$\boldsymbol{\nabla}\cdot\mathbf{v} = \frac{\partial u}{\partial x} + \frac{\partial v}{\partial y} = 0, \tag{8}$$

where u and v represent the x and y components of the velocity, respectively, i.e., $\mathbf{v} \equiv u\mathbf{1}_x + v\mathbf{1}_y$. Relation (8) implies a uniform density ρ_0 throughout the system for all time, if initially so, as well as the existence of a scalar function $\psi(x,y)$, known as the *stream function*, defined by the relations

$$u = \frac{\partial \psi}{\partial y}, \quad v = -\frac{\partial \psi}{\partial x}. \tag{9}$$

Scaling lengths by L_y, velocity by u_0, and time by L_y/u_0, the dimensionless equation for the stream function reads

$$\frac{\partial(\nabla^2\psi)}{\partial t} = -\frac{\partial\psi}{\partial y}\frac{\partial(\nabla^2\psi)}{\partial x} + \frac{\partial\psi}{\partial x}\frac{\partial(\nabla^2\psi)}{\partial y} + R^{-1}\nabla^2(\nabla^2\psi) + 8\pi^3 R^{-1}\cos(2\pi y), \tag{10}$$

where R is the Reynolds number,

$$R = \frac{\rho_0 u_0 L_y}{\eta}. \tag{11}$$

The stationary solution of Eq. (10) is

$$\psi_{st} = -\frac{1}{2\pi}\cos(2\pi y). \tag{12}$$

Setting $\psi = \psi_{st} + \delta\psi$ and linearizing Eq. (10) around ψ_{st}, one gets

$$\frac{\partial(\nabla^2\delta\psi)}{\partial t} = -\sin(2\pi y)\frac{\partial(\nabla^2\delta\psi)}{\partial x} - 4\pi^2\sin(2\pi y)\frac{\partial\delta\psi}{\partial x} + R^{-1}\nabla^2(\nabla^2\delta\psi). \tag{13}$$

Owing to periodic boundary conditions, $\delta\psi(x,y,t)$ can be expanded in Fourier series:

$$\delta\psi(x,y,t)=\sum_{k_x,\,k_y=-\infty}^{\infty}\exp(-2\pi i k_y y)\times\exp(-2\pi i k_x x/a_r)\,\delta\psi_{k_x,k_y}(t),$$
$$\delta\psi_{k_x,k_y}(t)=\int_0^1 dy\exp(2\pi i k_y y)\frac{1}{a_r}\int_0^{a_r}dx\times\exp(2\pi i k_x x/a_r)\,\delta\psi(x,y,t). \tag{14}$$

Equation (13) can then be transformed to

$$\frac{\partial\delta\psi_{k_x,k_y}}{\partial t}=-4\pi^2 R^{-1}(\tilde{k}_x^2+k_y^2)\delta\psi_{k_x,k_y}+\pi\tilde{k}_x[\delta\psi_{k_x,k_y+1}-\delta\psi_{k_x,k_y-1}]+2\pi\frac{\tilde{k}_x k_y}{\tilde{k}_x^2+k_y^2}[\delta\psi_{k_x,k_y+1}+\delta\psi_{k_x,k_y-1}], \tag{15}$$

where we have set

$$\tilde{k}_x=k_x/a_r. \tag{16}$$

In its general form, the analysis of this equation proves to be quite difficult [21]. On the other hand, if ψ_{st} is stable, then in the long time limit the evolution of the system will be mainly governed by long wavelength modes. Accordingly, we start our analysis by considering only the modes $k_y=0,\pm1$, i.e., we assume that $\delta\psi(k_x,k_y t)\approx0$ for $|k_y|\geqslant2$ [22]. Defining the vector $\boldsymbol{\delta\psi}_{k_x}\equiv(\delta\psi_{k_x,0},\delta\psi_{k_x,1},\delta\psi_{k_x,-1})$, Eq. (15) can be written in the following matrix form:

$$\frac{\partial\boldsymbol{\delta\psi}_{k_x}(t)}{\partial t}=\mathbf{A}\cdot\boldsymbol{\delta\psi}_{k_x}(t), \tag{17}$$

with

$$\mathbf{A}=\begin{pmatrix}-4\pi^2R^{-1}\tilde{k}_x^2 & \pi\tilde{k}_x & -\pi\tilde{k}_x\\ \pi\tilde{k}_x(1-\tilde{k}_x^2)/(1+\tilde{k}_x^2) & -4\pi^2R^{-1}(1+\tilde{k}_x^2) & 0\\ -\pi\tilde{k}_x(1-\tilde{k}_x^2)/(1+\tilde{k}_x^2) & 0 & -4\pi^2R^{-1}(1+\tilde{k}_x^2)\end{pmatrix}. \tag{18}$$

We first note that the matrix $\mathbf{A}$ is diagonal for $k_x=0$ so that the solution of Eq. (17) simply reduces to

$$\delta\psi_{0,1}(t)\sim\delta\psi_{0,-1}(t)\sim\exp(-4\pi^2R^{-1}t). \tag{19}$$

Furthermore, by definition of the stream function Eq. (9), $\psi_{0,0}(t)=0,\forall t$. We thus concentrate on the case $k_x\neq0$, looking for a similarity transformation $\mathbf{T}\cdot\mathbf{A}\cdot\mathbf{T}^{-1}$ that diagonalizes the matrix $\mathbf{A}$. After some algebra, one finds

$$\mathbf{T}=\begin{pmatrix}(\lambda_1-\lambda_3)/\pi\tilde{k}_x & 1 & -1\\ (\lambda_2-\lambda_3)/\pi\tilde{k}_x & 1 & -1\\ 0 & 1 & 1\end{pmatrix}, \tag{20}$$

where $\{\lambda_i\}$ are the eigenvalues of $\mathbf{A}$:

$$\lambda_1=-2\pi^2R^{-1}(1+2\tilde{k}_x^2)+\pi\sqrt{2\tilde{k}_x^2(1-\tilde{k}_x^2)/(1+\tilde{k}_x^2)+4\pi^2R^{-2}},$$
$$\lambda_2=-2\pi^2R^{-1}(1+2\tilde{k}_x^2)-\pi\sqrt{2\tilde{k}_x^2(1-\tilde{k}_x^2)/(1+\tilde{k}_x^2)+4\pi^2R^{-2}},$$
$$\lambda_3=-4\pi^2R^{-1}(1+\tilde{k}_x^2). \tag{21}$$

Equation (17) then becomes

$$\frac{\partial\delta\phi_i(t)}{\partial t}=\lambda_i\,\delta\phi_i(t),\ i=1,2,3, \tag{22}$$

where

$$\boldsymbol{\delta\phi}=\mathbf{T}\cdot\boldsymbol{\delta\psi}. \tag{23}$$

It follows from Eq. (21) that λ_2 and λ_3 are always negative, whereas there exists a critical value of the Reynolds number

$$R_c(k_x)=2\sqrt{2}\,\pi\frac{1+\tilde{k}_x^2}{\sqrt{1-\tilde{k}_x^2}},\quad 0<\tilde{k}_x^2<1, \tag{24}$$

for which λ_1 vanishes, thus indicating the limit of stability of the corresponding mode [23]. Clearly R_c is an increasing function of $|k_x|$, so that the first modes to become unstable correspond to $|k_x|=1$, provided the aspect ratio $a_r>1$. As $a_r\to1$, $R_c\to\infty$, indicating that no instability can develop for perturbations of the same spatial periodicity as the applied force [24]. In the following, we shall therefore concentrate mainly on the case $a_r>1$.

For $a_r=2$, relation (24) predicts a critical Reynolds number of $R_c\approx12.8255$. Analytical calculations can still be handled when the modes $k_y=\pm2$ are taken into account as well, and lead to

$$R_c^{(5)}(k_x)=R_c(k_x)\left[1+\frac{\tilde{k}_x^4\,(\tilde{k}_x^2+3)}{2\,(\tilde{k}_x^2+4)^2\,(\tilde{k}_x^2-1)}\right]^{-1/2},\quad 0<\tilde{k}_x^2<1. \tag{25}$$

For $a_r=2$, one finds a critical Reynolds number of $R_c^{(5)}\approx 12.8738$, so that the discrepancy remains below 0.4%. Numerical evaluation of R_c performed with a total of 103 modes shows no further significant discrepancy. We thus conclude that one can rely reasonably well on a three-mode approximation theory [that is, $\delta\psi_{k_x,k_y}(t)\approx 0$ for $|k_y|\geqslant 2$]. It remains to check whether this approximation leads to the correct velocity field beyond the instability. To this end we need to work out the explicit form of the stream function.

The calculations are tedious and quite lengthy, so that here we report only the basic steps. We start with the full nonlinear evolution equation for $\delta\psi=\psi-\psi_{st}$:

$$\begin{aligned}\frac{\partial(\nabla^2\delta\psi)}{\partial t}=&-\sin(2\,\pi y)\,\frac{\partial(\nabla^2\delta\psi)}{\partial x}-4\,\pi^2\sin(2\,\pi y)\,\frac{\partial\delta\psi}{\partial x}\\&+R^{-1}\,\nabla^2(\nabla^2\delta\psi)-\frac{\partial\delta\psi}{\partial y}\,\frac{\partial(\nabla^2\delta\psi)}{\partial x}\\&+\frac{\partial\delta\psi}{\partial x}\,\frac{\partial(\nabla^2\delta\psi)}{\partial y}.\end{aligned} \tag{26}$$

As for the linear case, we take the Fourier transform of this equation, limiting ourselves to the first three modes $k_y=0,\pm 1$. Applying then the transformation $\mathbf{T}$ to the resulting equation [cf. Eq. (23)], one obtains

$$\frac{\partial\delta\phi_i(t)}{\partial t}=\lambda_i\,\delta\phi_i(t)+\Phi_i,\quad i=1,2,3, \tag{27}$$

where the Φ_i's are nonlinear polynomial functions of $\delta\phi_1$, $\delta\phi_2$, and $\delta\phi_3$ and their complex-conjugates. Close to the bifurcation point ($R\approx R_c$, $k_x=1$), the mode $\delta\phi_1$ exhibits a *critical slowing down* since $\lambda_1(k_x=1)\approx 0$. On this slow time scale, i.e., $t\approx O(\lambda_1^{-1})$, the fast modes $\delta\phi_2$ and $\delta\phi_3$ can be considered as stationary, their time dependence arising mainly through $\delta\phi_1(t)$. Setting $\partial\delta\phi_2/\partial t\approx\partial\delta\phi_3/\partial t\approx 0$, one can express the fast modes $\delta\phi_2$ and $\delta\phi_3$ in terms of the slow mode $\delta\phi_1$ and its complex conjugate, $\delta\phi_1^*$. If now one inserts the expressions thus obtained for the fast modes into the evolution equation of the slow mode, one obtains a closed nonlinear equation for the latter (*adiabatic elimination* [25,26]). In practice, however, such a calculation is possible only close to the bifurcation point, where the amplitude of $\delta\phi_1$ is supposed to approach zero as $R\to R_c$. In fact, there exist other types of transitions, such as the one arising in the Vanderpol equation, where the amplitude of the solution above the instability does not vanish as one approaches the critical point [27]. Detailed analysis shows that this is not the case here (i.e., $|\delta\phi_1|\to 0$ as $R\to R_c$), so that we can limit ourselves to lowest orders in $|\delta\phi_1|$, obtaining finally the so-called *normal form* or *amplitude equation* for the slow mode:

$$\begin{aligned}\frac{\partial\delta\phi_1(t)}{\partial t}=&\lambda\,\delta\phi_1(t)-\gamma\,|\delta\phi_1(t)|^2\,\delta\phi_1(t)\\&\times[1+O(|\delta\phi_1(t)|^2)],\end{aligned} \tag{28}$$

where

$$\begin{aligned}\lambda\equiv&\lambda_1(k_x=1)\\=&\frac{4\pi^2}{R}\,\frac{a_r^2+1}{a_r^2(a_r^2+2)}\left(1-\frac{R_c^2}{R^2}\right)+O(|R/R_c-1|^2)\end{aligned} \tag{29}$$

and γ is a positive constant whose expression, to dominant order in $|R/R_c-1|$, is given by

$$\gamma=8\,\sqrt{2}\,\pi^3\frac{(a_r^6+17\,a_r^4+16\,a_r^2-32)\,(a_r^2+1)^2}{a_r^3\,(a_r^2-1)^{3/2}(a_r^2+2)^3\,(a_r^2+4)^2}. \tag{30}$$

Above the bifurcation point $R>R_c$ ($\lambda>0$), the amplitude equation (28) admits two stable stationary solutions, corresponding to the rotation sense of the streamlines in the fluid:

$$\delta\phi_1^{\pm}=\pm\sqrt{\frac{\lambda}{\gamma}}\exp(i\,\theta_0), \tag{31}$$

where θ_0 is a constant whose value depends on the initial conditions. The fact that the stationary solution still depends on the initial conditions simply reflects the Galilean invariance in the x direction that results from the periodic boundary conditions imposed on the system. Using relation (31), one can compute the explicit form of the fast modes for $k_x=0,\pm 1,\pm 2$. Applying the inverse transform $\mathbf{T}^{-1}(k_x)$ [cf. Eq. (20)], to the vector $\boldsymbol{\delta\phi}^{\pm}(k_x)=(\delta\phi_1^{\pm},\delta\phi_2^{\pm},\delta\phi_3^{\pm})$ obtained and taking its inverse Fourier transform, one gets the explicit expression of the stream function in real space. Up to order $O(R/R_c-1)$, one obtains

$$\begin{aligned}\psi_{st}^{\pm}(x,y)=&-\frac{1}{2\,\pi}\cos(2\,\pi y)\pm\frac{R_c\,a_r}{2\,\pi\,(a_r^2+2)}\,|\delta\phi_1|\\&\times\left[\cos(2\pi x/a_r-\theta_0)-\frac{4\,\pi}{a_r\,R_c}\sin(2\pi x/a_r\right.\\&\left.-\theta_0)\sin(2\pi y)\right]+\frac{R_c^2}{2\,\pi\,(a_r^2+2)^2}\,|\delta\phi_1|^2\\&\times\left[1-\frac{a_r^4}{(a_r^2+4)^2}\cos(4\pi x/a_r-2\theta_0)\right]\cos(2\pi y),\end{aligned} \tag{32}$$

where we have set $|\delta\phi_1|\equiv|\delta\phi_1^{\pm}|$. Using the relations (9), the velocity profiles can now be obtained straightforwardly:

$$\begin{aligned}u_{st}^{\pm}(x,y)=&\sin(2\pi y)\mp\frac{4\,\pi}{(a_r^2+2)}\,|\delta\phi_1|\,\sin(2\pi x/a_r-\theta_0)\\&\times\cos(2\pi y)-\frac{R_c^2}{(a_r^2+2)^2}\,|\delta\phi_1|^2\left[1-\frac{a_r^4}{(a_r^2+4)^2}\right.\\&\left.\times\cos(4\pi x/a_r-2\theta_0)\right]\sin(2\pi y),\end{aligned} \tag{33}$$

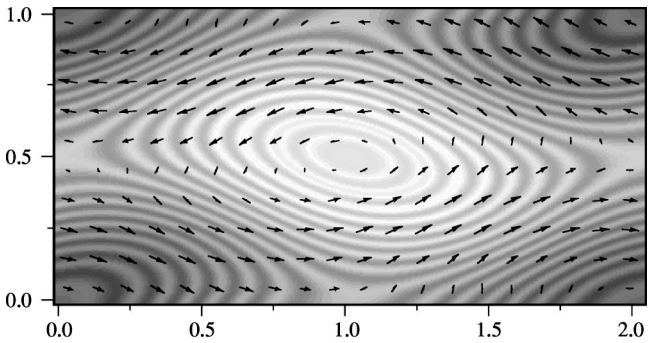

FIG. 1. Density plot of the stream function Eq. (32) for $R=15$, $a_r=2$, and $\theta_0=0$. For the sake of clarity, a vector plot of the velocity field is also included.

$$v_{st}^{\pm}(x,y)=\pm\frac{R_c}{(a_r^2+2)}|\delta\phi_1|\left[\sin(2\pi x/a_r-\theta_0)+\frac{4\pi}{a_r R_c}\cos(2\pi x/a_r-\theta_0)\sin(2\pi y)\right]-\frac{2R_c^2 a_r^3}{(a_r^2+2)^2(a_r^2+4)^2}|\delta\phi_1|^2\times\sin(4\pi x/a_r-2\theta_0)\cos(2\pi y). \quad (34)$$

A density plot of the stream function (32) is represented in Fig. 1 for $R=15$, $a_r=2$, and $\theta_0=0$, where, for the sake of clarity, a vector plot of the velocity field is also included. We note that the flow has an ABC-like topology [28], with closed streamlines (eddies), open ones, and separatrices between them.

We recall that the above results rest on the three-mode approximation theory. To check the validity of this basic assumption, we have solved numerically the incompressible nonlinear hydrodynamic equations for $a_r=2$, using standard techniques [29]. Figure 2 compares contour plots of the stream function obtained numerically with its corresponding theoretical counterpart Eq. (32) for $R=15$. Given the relatively large distance from the critical point $(R/R_c-1\approx 17\%)$, the agreement is much better than expected, the discrepancy remaining below 5%. Surprisingly, the agreement does not improve as we consider smaller values of the

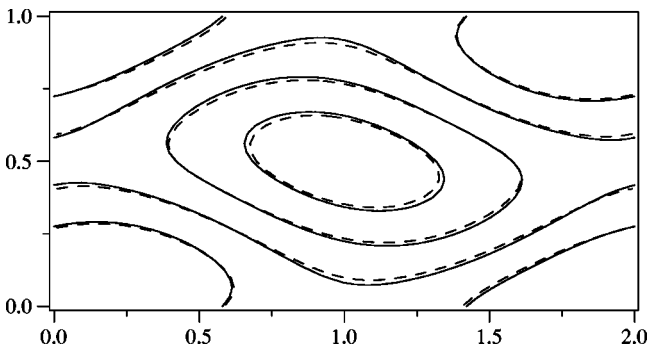

FIG. 2. Stationary state contour plot of the stream function for $R=15$, $a_r=2$, and $\theta_0=0$. The full and dashed lines correspond to theoretical prediction [Eq. (32)] and numerical results, respectively. The discrepancy remains below 5%.

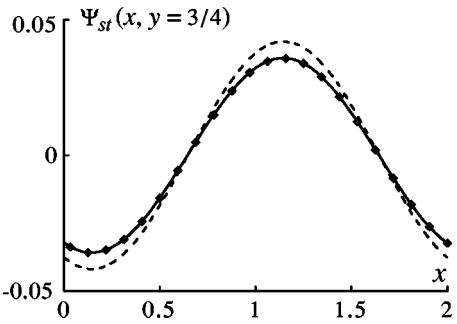

FIG. 3. Horizontal profile of the stationary state stream function, with $y=3/4$, as a function of the coordinate x for $R=13$, $a_r=2$, and $\theta_0=0$. The full and dashed lines represent theoretical predictions obtained by using an estimation of the critical Reynolds number based on five-mode [Eq. 25)] and three-mode [Eq. 24)] approximation theories, respectively. The diamonds correspond to numerical results.

Reynolds number [30]. This is shown in Fig. 3, where both the numerical and the theoretical horizontal profiles of the stream function with a fixed value of the vertical coordinate $y=3/4$ are depicted for the Reynolds number $R=13$. The discrepancy now exceeds 10%.

To understand the origin of this unexpected behavior, we note that the value of the critical Reynolds number that we have used to evaluate the stream function [Eq. (32)] is based on the three-mode approximation theory [cf. Eq. (24)]. As shown before, the accuracy of the latter value of R_c is about 0.4%, which is fine as long as the distance from the critical point (R/R_c-1) remains much larger than 0.4%. Now, for $R=13$, the distance from the critical point is about 1%, which is of the same order as the accuracy of R_c and explains the relatively important discrepancy we observe in Fig. 3.

To overcome this difficulty, one has to compute a more accurate value of the critical Reynolds number, based, for instance, on the five-mode approximation theory [cf. Eq. (25)]. As is well known [26], this correction concerns only the value of R_c, and in no way compromises the validity of the amplitude equation (28) and its corresponding solution Eq. (32). This is illustrated in Fig. 3, where excellent agreement with the numerical result is demonstrated, whenever we use $R_c^{(5)}$ as the critical Reynolds number. For smaller values of R, one can compute the value of R_c numerically with the desired precision and use it as an input to the amplitude equation (28).

So far, we have limited ourselves to the analysis of the deterministic equations only, i.e., we have discarded the noise terms. In principle, there is no difficulty in taking into account the noise contributions as well, except that the amplitudes of the field variables $(\delta\phi_1,\delta\phi_2,\delta\phi_3)$ are now directly related to the amplitude $\mathcal{B}$ of the noise, which is typically a small parameter. For example, the fast variables $(\delta\phi_2,\delta\phi_3)\approx O(\mathcal{B}^{1/2})$, whereas the slow variable $\delta\phi_1\approx O(\mathcal{B}^{1/4})$ (a detailed discussion of this problem is given in [31]). Keeping this restriction in mind, one can repeat all the above calculations in the presence of noise terms. To the dominant order in $|\delta\phi_1|$, one finds

$$\frac{\partial\delta\phi_1(t)}{\partial t}=\lambda\,\delta\phi_1(t)-\gamma|\delta\phi_1(t)|^2\,\delta\phi_1(t)+\xi(t),$$

$$\frac{\partial \delta\phi_1^*(t)}{\partial t} = \lambda\ \delta\phi_1^*(t) - \gamma\,|\delta\phi_1(t)|^2\ \delta\phi_1^*(t) + \xi^*(t). \tag{35}$$

The function $\xi(t)$ and its complex conjugate $\xi^*(t)$ are Gaussian white noises with zero means and correlations given by

$$\langle \xi(t)\ \xi(t')\rangle = 0,$$
$$\langle \xi(t)\ \xi^*(t')\rangle = \mathcal{B}\,\delta(t-t'), \tag{36}$$

with

$$\mathcal{B} = \frac{4\,k_B\,T_0\,a_r^2}{M\,u_0^2\,R}[1 + O(|R/R_c - 1|)], \tag{37}$$

M being the total mass of the system:

$$M = a_r \rho_0 L_y^2. \tag{38}$$

The results derived in this section were based explicitly on the incompressibility assumption. However, as discussed in the Introduction, this assumption is inconsistent with the very foundation of the fluctuating hydrodynamic formalism. On the other hand, we have presented in [1] numerical evidence that in the vicinity of the bifurcation point the system behaves essentially as an incompressible fluid. We therefore expect that the Langevin equation (35) should remain valid for R close enough to R_c. We shall clarify this major issue in the next section.

III. FLUCTUATIONS IN THE COMPRESSIBLE FLOW

Let us now consider the compressible hydrodynamic equations (3)–(5), for which we need to specify an equation of state. Since the system is isothermal, we simply set

$$p = c_s^2\,\rho, \tag{39}$$

where c_s is the isothermal speed of sound. As in the previous section, we start with the linearized hydrodynamic equations around the reference state $\{\rho_0, \mathbf{v}_{st}\}$, where $\mathbf{v}_{st}$ is given by Eq. (7). Setting

$$\rho = \rho_0 + \delta\rho,$$
$$\mathbf{v} = \mathbf{v}_{st} + \delta\mathbf{v}, \tag{40}$$

and scaling lengths by L_y, time by L_y/c_s, $\delta\rho$ by ρ_0, and $\delta\mathbf{v}$ by the speed of sound c_s, the dimensionless linear fluctuating equations in Fourier space read (recall that $\tilde{k}_x \equiv k_x/a_r$)

$$\frac{\partial\,\delta\rho_{k_x,k_y}(t)}{\partial t} = 2\,\pi\,i\,(\tilde{k}_x\,\delta u_{k_x,k_y} + k_y\,\delta v_{k_x,k_y}) + \varepsilon\,R\,\pi\,\tilde{k}_x\,(\delta\rho_{k_x,k_y+1} - \delta\rho_{k_x,k_y-1}), \tag{41}$$

$$\frac{\partial \delta u_{k_x,k_y}(t)}{\partial t} = -\pi\,\varepsilon\,R(\delta v_{k_x,k_y+1} + \delta v_{k_x,k_y-1}) + \pi\,\varepsilon\,R\,\tilde{k}_x\,(\delta u_{k_x,k_y+1} - \delta u_{k_x,k_y-1}) - 4\,\pi^2\,\varepsilon(\tilde{k}_x^2 + k_y^2)\,\delta u_{k_x,k_y} - 4\,\pi^2\,\alpha\,\varepsilon\,\tilde{k}_x(\tilde{k}_x\,\delta u_{k_x,k_y} + k_y\,\delta v_{k_x,k_y}) + 2\,\pi\,i\,\tilde{k}_x\,\delta\rho_{k_x,k_y} + F_{k_x,k_y}(t), \tag{42}$$

$$\frac{\partial \delta v_{k_x,k_y}(t)}{\partial t} = \pi\,\varepsilon\,R\,\tilde{k}_x\,(\delta v_{k_x,k_y+1} - \delta v_{k_x,k_y-1}) - 4\,\pi^2\,\varepsilon(\tilde{k}_x^2 + k_y^2)\,\delta v_{k_x,k_y} - 4\,\pi^2\,\alpha\,\varepsilon\,k_y\,(\tilde{k}_x\,\delta u_{k_x,k_y} + k_y\,\delta v_{k_x,k_y}) + 2\,\pi\,i\,k_y\,\delta\rho_{k_x,k_y} + G_{k_x,k_y}(t), \tag{43}$$

where R is the Reynolds number, defined in Eq. (11),

$$\varepsilon = \frac{\eta}{\rho_0\,c_s\,L_y}, \tag{44}$$

and

$$\alpha = \zeta/\eta. \tag{45}$$

The functions F_{k_x,k_y} and G_{k_x,k_y} are Fourier components of the noise terms; their covariances follow directly from Eqs. (5) and (6):

$$\langle F_{k_x,k_y}(t)\,F_{k_x',k_y'}(t')\rangle = 8\,\pi^2\,\varepsilon\,\mathcal{A}[(\alpha+1)\,\tilde{k}_x^2 + k_y^2]\,\delta^{Kr}_{\mathbf{k}+\mathbf{k}',0}\,\delta(t-t'),$$

$$\langle F_{k_x,k_y}(t)\,G_{k_x',k_y'}(t')\rangle = 8\,\pi^2\,\varepsilon\,\mathcal{A}\,\alpha\,\tilde{k}_x\,k_y\,\delta^{Kr}_{\mathbf{k}+\mathbf{k}',0}\,\delta(t-t'),$$

$$\langle G_{k_x,k_y}(t)\,G_{k_x',k_y'}(t')\rangle = 8\,\pi^2\,\varepsilon\,\mathcal{A}[\tilde{k}_x^2 + (\alpha+1)\,k_y^2] \times \delta^{Kr}_{\mathbf{k}+\mathbf{k}',0}\,\delta(t-t'), \tag{46}$$

where $\mathbf{k} \equiv (\tilde{k}_x, k_y)$ and

$$\mathcal{A} = \frac{k_B\,T_0}{M\,{c_s}^2}, \tag{47}$$

M being the total mass of the system [cf. Eq. (38)].

For the sake of clarity, we first focus on the *deterministic* behavior, i.e., we discard for the moment the noise contributions from the evolution equations (41)–(43). Furthermore, we shall limit ourselves to the three-mode approximation theory, i.e., we shall neglect the modes with $|k_y| \geqslant 2$, for the very same reasons that we have discussed for the incompressible case. With these assumptions, Eqs. (41)–(43) reduce to a system of nine coupled equations. It can then be checked that the change of variables

$$\delta\rho^{\pm}_{k_x}(t)=\delta\rho_{k_x,1}(t)\pm\delta\rho_{k_x,-1}(t),$$
$$\delta u^{\pm}_{k_x}(t)=\delta u_{k_x,1}(t)\pm\delta u_{k_x,-1}(t), \quad (48)$$
$$\delta v^{\pm}_{k_x}(t)=\delta v_{k_x,1}(t)\pm\delta v_{k_x,-1}(t)$$

leads to a ''partial diagonalization'' of the evolution equations, i.e., the equations for the variables $\{\delta\rho_{k_x,0},\ \delta\rho^{-}_{k_x},\ \delta u_{k_x,0},\ \delta u^{-}_{k_x},\ \delta v^{+}_{k_x}\}$ decouple from the rest. Furthermore, their associated eigenvalues prove to remain strictly negative, regardless of the value of the Reynolds number R, so that they are not determinant for the onset of convective instability. We therefore focus on the remaining four variables $\{\delta\rho^{+}_{k_x},\delta u^{+}_{k_x},\delta v^{-}_{k_x},\delta v_{k_x,0}\}$. Defining the vector $\delta\mathbf{h}_{k_x}(t)\equiv\{\delta\rho^{+}_{k_x},\ \delta u^{+}_{k_x},\ \delta v^{-}_{k_x},\ \delta v_{k_x,0}\}$ one readily finds

$$\frac{\partial}{\partial t}\delta\mathbf{h}_{k_x}(t)=\mathbf{C}(k_x)\cdot\delta\mathbf{h}_{k_x}(t), \quad (49)$$

where the matrix $\mathbf{C}$ is given by

$$\mathbf{C}(k_x)=\begin{pmatrix} 0 & 2\pi i\tilde{k}_x & 2\pi i & 0 \\ 2\pi i\tilde{k}_x & -4\pi^2\varepsilon(1+\alpha\tilde{k}_x^2+\tilde{k}_x^2) & -4\pi^2\varepsilon\alpha\tilde{k}_x & -2\pi\varepsilon R \\ 2\pi i & -4\pi^2\varepsilon\alpha\tilde{k}_x & -4\pi^2\varepsilon(1+\alpha+\tilde{k}_x^2) & -2\pi\varepsilon\tilde{k}_x R \\ 0 & 0 & \pi\varepsilon\tilde{k}_x R & -4\pi^2\varepsilon\tilde{k}_x^2 \end{pmatrix}. \quad (50)$$

The analysis can be simplified somewhat by noticing that the parameter ε must remain small if one wishes to remain within the limit of validity of the hydrodynamic regime [32]. Furthermore, as already mentioned in the introduction, in this article we limit ourselves to strictly subsonic flows, so that we shall restrict the analysis to a parameter domain where

$$\varepsilon\ll 1,\ \varepsilon R=u_0/c_s\ll 1. \quad (51)$$

Accordingly, we evaluate the eigenvalues of the matrix $\mathbf{C}$ perturbatively:

$$\tilde{\lambda}(k_x)=\tilde{\lambda}^{(0)}(k_x)+\varepsilon\,\tilde{\lambda}^{(1)}(k_x)+\ldots. \quad (52)$$

After some algebra, one finds, up to order $O(\varepsilon^2)$,

$$\tilde{\lambda}_1(k_x)=\varepsilon[-2\,\pi^2(1+2\tilde{k}_x^2)+\pi\sqrt{4\,\pi^2+2\,R^2\tilde{k}_x^2\,(1-\tilde{k}_x^2)/(1+\tilde{k}_x^2)}],$$
$$\tilde{\lambda}_2(k_x)=\varepsilon[-2\,\pi^2(1+2\tilde{k}_x^2)-\pi\sqrt{4\,\pi^2+2\,R^2\tilde{k}_x^2\,(1-\tilde{k}_x^2)/(1+\tilde{k}_x^2)}], \quad (53)$$
$$\tilde{\lambda}_3(k_x)=2\,\pi\,i\sqrt{1+\tilde{k}_x^2}-2\,\pi^2(\alpha+1)\,\varepsilon(1+\tilde{k}_x^2),$$
$$\tilde{\lambda}_4(k_x)=-2\,\pi\,i\sqrt{1+\tilde{k}_x^2}-2\,\pi^2(\alpha+1)\,\varepsilon(1+\tilde{k}_x^2).$$

The eigenvalues $\tilde{\lambda}_1$ and $\tilde{\lambda}_2$ correspond to dissipative (viscous) modes, while $\tilde{\lambda}_3$ and $\tilde{\lambda}_4$ are related to the propagation of (damped) sound waves. It can then be easily checked that the real parts of $\tilde{\lambda}_2$, $\tilde{\lambda}_3$, and $\tilde{\lambda}_4$ are always negative, whereas there exists a critical value of the Reynolds number

$$R_c(k_x)=2\sqrt{2}\,\pi\frac{1+\tilde{k}_x^2}{\sqrt{1-\tilde{k}_x^2}},\quad 0<\tilde{k}_x^2<1, \quad (54)$$

for which $\tilde{\lambda}_1$ vanishes, thus indicating the limit of stability of the corresponding mode.

Remarkably, the above expression for the critical Reynolds number is identical to the one obtained in the incompressible case [cf. Eq. (24)]. In fact, detailed analysis shows that the relation (54) is exact, i.e., it is independent of ε, at least within the framework of the three-mode approximation theory. On the other hand, if the modes $k_y=\pm 2$ are taken into account as well, tedious calculations lead to

$$R_c^{(5)}(k_x)=R_c(k_x)\left[1+\frac{\tilde{k}_x^4(\tilde{k}_x^2+3)}{2(\tilde{k}_x^2+4)^2(\tilde{k}_x^2-1)}\right]^{-1/2}+\mathcal{O}((u_0/c_s)^2),\quad 0<\tilde{k}_x^2<1, \quad (55)$$

which is again equivalent to the corresponding result obtained for the incompressible case, Eq. (25), the correction being of the order of $O(\varepsilon^2)$. In particular, the first mode to become unstable corresponds to $|k_x|=1$, provided $a_r>1$.

We note that the matrix $\mathbf{C}$ is singular for $k_x=0$, i.e., one of its eigenvalues vanishes. A close inspection shows that this zero eigenvalue corresponds to the mode $\delta v_{0,0}$, which is identically zero because of linear momentum conservation. Accordingly, in what follows we shall concentrate on the case $k_x\neq 0$, looking for a similarity transformation $\mathbf{S}\cdot\mathbf{C}\cdot\mathbf{S}^{-1}$ that diagonalizes the matrix $\mathbf{C}$. For consistency, here again we perform the calculations perturbatively, i.e., we expand $\mathbf{S}$ in powers of ε:

$$\mathbf{S}(k_x)=\mathbf{S_0}(k_x)+\varepsilon\,\mathbf{S_1}(k_x)+\cdots. \quad (56)$$

Note that this method constitutes an alternative to the time scale perturbation theory [33] that was generalized by Schmitz and Cohen [15] in order to study the Bénard instability in a compressible fluid.

Since the explicit form of the eigenvalues is known up to $O(\varepsilon^2)$, we need to evaluate $\mathbf{S}$ (and its inverse $\mathbf{S}^{-1}$) only up to the same order. Despite this simplification, the general expression for $\mathbf{S}$ is quite awkward and will not be presented here. The rest of the calculations are quite straightforward, but remain tedious and lengthy, so we give only a brief sketch of the basic steps [see the discussion below Eq. (27)].

We start by taking the Fourier transform of the fluctuating hydrodynamic equations (3)–(5). Using the change of variables (40) and (48), we next derive the nonlinear fluctuating equations for $\delta\mathbf{h}_{k_x}$. We then apply the transformation $\mathbf{S}$ to the latter, obtaining a set of four nonlinear equations for the variables $\{\delta\tilde{\phi}_1,\delta\tilde{\phi}_2,\delta\tilde{\phi}_3,\delta\tilde{\phi}_4\}\equiv\delta\tilde{\boldsymbol{\phi}}(t)=\mathbf{S}\cdot\delta\mathbf{h}_{k_x}$. Close to the bifurcation point ($R\approx R_c$, $k_x=1$), the mode $\delta\tilde{\phi}_1$ exhibits a critical slowing down, since by construction $\tilde{\lambda}_1\approx 0$. We can therefore proceed to an adiabatic elimination of the fast modes $\{\delta\tilde{\phi}_2,\delta\tilde{\phi}_3,\delta\tilde{\phi}_4\}$, limiting ourselves to dominant orders in $|\delta\tilde{\phi}_1|$ [see the paragraph preceding Eq. (35)]. The final result is a set of two coupled Langevin equations for the slow mode $\delta\tilde{\phi}_1$ and its complex conjugate $\delta\tilde{\phi}_1^*$:

$$\frac{\partial\delta\tilde{\phi}_1(t)}{\partial t}=\tilde{\lambda}\,\delta\tilde{\phi}_1(t)-\tilde{\gamma}\,|\delta\tilde{\phi}_1(t)|^2\,\delta\tilde{\phi}_1(t)+\tilde{\xi}(t),$$
$$\frac{\partial\delta\tilde{\phi}_1^*(t)}{\partial t}=\tilde{\lambda}\,\delta\tilde{\phi}_1^*(t)-\tilde{\gamma}\,|\delta\tilde{\phi}_1(t)|^2\,\delta\tilde{\phi}_1^*(t)+\tilde{\xi}^*(t), \tag{57}$$

with

$$\tilde{\lambda}=\tilde{\lambda}_1(k_x=1)=\lambda\,\frac{u_0}{c_s}[1+\mathcal{O}(u_0^2/c_s^2)]$$
$$\approx 4\pi^2\varepsilon\,\frac{a_r^2+1}{a_r^2(a_r^2+2)}\left(1-\frac{R_c^2}{R^2}\right) \tag{58}$$

and

$$\tilde{\gamma}=\gamma\,\frac{c_s}{u_0}[1+\mathcal{O}(u_0^2/c_s^2)\,]\approx\frac{\gamma}{\varepsilon R}, \tag{59}$$

where λ and γ are given by Eqs. (29) and (30), respectively. The function $\tilde{\xi}(t)$ and its complex conjugate $\tilde{\xi}^*(t)$ are Gaussian white noises with zero means and correlations given by

$$\langle\tilde{\xi}(t)\,\tilde{\xi}(t')\rangle=0,$$
$$\langle\tilde{\xi}(t)\,\tilde{\xi}^*(t')\rangle=\tilde{\mathcal{B}}\,\delta(t-t'), \tag{60}$$

with

$$\tilde{\mathcal{B}}=\left(\frac{u_0}{c_s}\right)^3\mathcal{B}[1+\mathcal{O}(u_0^2/c_s^2)]\approx 4\,\varepsilon\,a_r^2\,\mathcal{A}, \tag{61}$$

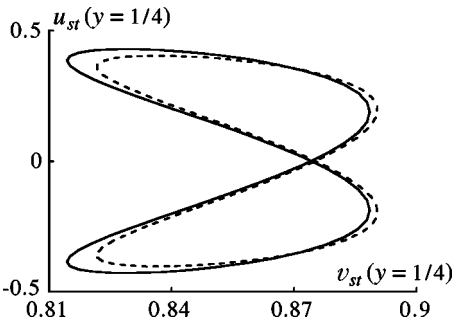

FIG. 4. Horizontal versus vertical components of the stationary state velocity field with $y=1/4$. The full line corresponds to theoretical predictions, as given by Eqs. (33) and (34), whereas the dashed line is obtained by solving numerically the compressible nonlinear hydrodynamic equations. The parameters are $R=15$, $a_r=2$, $\theta_0=0$, and $\varepsilon=10^{-2}$. The discrepancy is about 5%.

where $\mathcal{B}$ and $\mathcal{A}$ are given by Eqs. (37) and (47), respectively.

Although the form of the Langevin equations (57) is the same as that obtained for the incompressible case, Eqs. (35), they are nevertheless not equivalent since their coefficients are clearly different, even to dominant order in ε. The main reason for this apparent discrepancy is related to the fact that, for the incompressible case, the analysis has been carried out by scaling the velocities by u_0, whereas for the compressible case we used a different scaling, i.e., we scaled the velocities by the velocity of sound c_s. If now we switch back to the former scaling, i.e., we perform the change of variables $t\rightarrow tc_s/u_0$, $\{u,v\}\rightarrow u_0/c_s\{u,v\}$, then Eqs. (57) lead to

$$\delta\tilde{\phi}_1(t)=\frac{u_0}{c_s}\,\delta\phi_1(t)[1+\mathcal{O}(u_0^2/c_s^2)\,]. \tag{62}$$

Remarkably, this result shows that, to dominant order in ε, the evolution of fluctuating compressible and incompressible hydrodynamic equations is governed by the very same slow mode, at least for values of Reynolds number close to its critical value.

Let us first consider the macroscopic behavior. Using Eqs. (58), (59), and (62), one can go backward step by step and derive as well the evolution equations of the hydrodynamic velocities near the instability threshold. It can then be easily checked that, to dominant order in ε, the compressible stationary velocity profiles are given by their incompressible expressions, Eqs. (33) and (34). To check this important result, we have solved numerically the full nonlinear compressible hydrodynamic equations and compared the result with analytical expressions obtained for the incompressible case. A typical result is shown in Fig. 4, where $u_{st}(x,y=1/4)$ as a function of $v_{st}(x,y=1/4)$ is depicted for $R=15$, $\varepsilon=10^{-2}$, and $a_r=2$. Given the relatively large values of the Reynolds number ($R/R_c-1\approx 17\%$) and ε, the agreement is very good, the discrepancy remaining below 5%.

We now concentrate on the behavior of fluctuations, as described by the Langevin equations (57). The associated Fokker-Planck equation reads

$$\frac{\partial P(\delta\tilde{\phi}_1,\delta\tilde{\phi}_1^*,t)}{\partial t} = \frac{\partial}{\partial(\delta\tilde{\phi}_1)}\left[-(\tilde{\lambda}\,\delta\tilde{\phi}_1-\tilde{\gamma}\delta\tilde{\phi}_1^2\,\delta\tilde{\phi}_1^*)\,P+\frac{\tilde{\mathcal{B}}}{2}\frac{\partial P}{\partial(\delta\tilde{\phi}_1^*)}\right] + \frac{\partial}{\partial(\delta\tilde{\phi}_1^*)}\left[-(\tilde{\lambda}\,\delta\tilde{\phi}_1^*-\tilde{\gamma}\delta\tilde{\phi}_1\,\delta\tilde{\phi}_1^{*2})\,P+\frac{\tilde{\mathcal{B}}}{2}\frac{\partial P}{\partial(\delta\tilde{\phi}_1)}\right]. \tag{63}$$

At the stationary state, one finds

$$P_{st}(\delta\tilde{\phi}_1,\delta\tilde{\phi}_1^*)=\mathcal{N}^{-1}\exp\left[\frac{2}{\tilde{\mathcal{B}}}\left(\tilde{\lambda}|\delta\tilde{\phi}_1|^2-\frac{\tilde{\gamma}}{2}|\delta\tilde{\phi}_1|^4\right)\right] \tag{64}$$

with

$$\mathcal{N}=\frac{1}{4}\sqrt{\pi\,\tilde{\mathcal{B}}/\tilde{\gamma}}\exp(\tilde{\lambda}^2/\,\tilde{\gamma}\tilde{\mathcal{B}})\ \mathrm{erfc}(-\tilde{\lambda}/\sqrt{\tilde{\gamma}\,\tilde{\mathcal{B}}}), \tag{65}$$

where $\mathrm{erfc}(\cdots)$ stands for the complementary error function. Thanks to this result, one readily gets

$$\langle|\delta\tilde{\phi}_1|^2\rangle=\frac{1}{\tilde{\gamma}}(\tilde{\lambda}+\tilde{\mathcal{B}}/4\mathcal{N}). \tag{66}$$

Away from the bifurcation point ($\tilde{\lambda}\ll 0$) the quartic term in Eq. (64) is negligible so that the distribution is Gaussian and

$$\langle|\delta\tilde{\phi}_1|^2\rangle_G\approx\frac{\mathcal{A}R^2\,a_r^4\,(a_r^2+2)}{2\,\pi^2(R_c^2-R^2)(a_r^2+1)}. \tag{67}$$

The fluctuations thus behave as $|\delta\tilde{\phi}_1|\approx\mathcal{O}(\mathcal{A}^{1/2})$. Recall that the parameter $\mathcal{A}$ is inversely proportional to the system's total number of particles so that $\mathcal{A}\ll 1$ [cf. Eq. (47)]. As one approaches the bifurcation point, the Gaussian character of the distribution is gradually lost. Right at the bifurcation point $\tilde{\lambda}=0$, one has

$$\langle|\delta\tilde{\phi}_1|^2\rangle_{\tilde{\lambda}=0}=2\,\varepsilon\,a_r\left(\frac{R_c\,\mathcal{A}}{\gamma\,\pi}\right)^{1/2}, \tag{68}$$

which shows that the fluctuations now behave as $|\delta\tilde{\phi}_1|\approx\mathcal{O}(\mathcal{A}^{1/4})$. The enhancement of fluctuations and the change of the probability law at the bifurcation point are a direct manifestation of spatial symmetry breaking associated with the emergence of convective patterns.

On the other hand, the fast modes $\{\delta\tilde{\phi}_2,\delta\tilde{\phi}_3,\delta\tilde{\phi}_4\}$ prove to remain Gaussian, regardless of the value of the Reynolds number. Detailed analysis shows that their contribution to nonequilibrium statistical properties of the fluid remain of the order of $\mathcal{O}(u_0^2/c_s^2)$. In other words, the fluctuation spectrum of hydrodynamic variables is mainly determined by the statistical properties of $\delta\tilde{\phi}_1$. For instance, the static velocity autocorrelation function is found to obey

$$\langle\delta\mathbf{v}_\mathbf{k}\cdot\delta\mathbf{v}_{-\mathbf{k}}\rangle-2\mathcal{A}=\frac{\pi^2(a_r^2+1)}{a_r^2\,(a_r^2+2)^2}\langle|\delta\tilde{\phi}_1|^2\rangle\times[1+\mathcal{O}((u_0/c_s)^2)], \tag{69}$$

where the second term on the left hand side is the equilibrium contribution and $\langle|\delta\tilde{\phi}_1|^2\rangle$ is given by Eq. (66).

It is instructive to study the Gaussian limit $R\ll R_c$, where the linearized Langevin equations, Eqs. (41)–(43), remain valid. As was shown in [1], they lead to the following expression for the static velocity autocorrelation function:

$$\langle\delta\mathbf{v}_\mathbf{k}\cdot\delta\mathbf{v}_{-\mathbf{k}}\rangle_G-2\mathcal{A}=\frac{\mathcal{A}R^2\,a_r^2}{2(R_c^2-R^2)(a_r^2+2)}. \tag{70}$$

Now, inserting into Eq. (69) the Gaussian form of $\langle|\delta\tilde{\phi}_1|^2\rangle$, as given by Eq. (67), leads precisely to the very same result. We thus conclude that our general expression Eq. (69) remains valid in the Gaussian regime $R\ll R_c$, despite the fact that it was derived in the close vicinity of the bifurcation point $R\approx R_c$.

To check the validity of our theoretical results, we have simulated the nonlinear fluctuating hydrodynamic equations (3)–(5) for different values of R, setting $a_r=2$, $\varepsilon=10^{-2}$, and $\mathcal{A}=10^{-3}/256\approx 3.9\times10^{-6}$. The estimated statistical errors remain below 5% for $R\leqslant 10$, but grow rapidly as we consider higher values of R, reaching about 13% for $R\approx R_c$. Above the bifurcation point, $R>R_c$, the stationary distribution has two maxima, located at $\delta\tilde{\phi}_1=\pm\sqrt{\tilde{\lambda}/\tilde{\gamma}}$, which correspond (up to a phase factor) to the deterministic stationary solutions of the amplitude equation (31). Because of the presence of noise terms, the system visits these states in a rather random fashion, resulting in a huge dispersion of data. This is especially true for R close to R_c, which is precisely the situation where our theoretical predictions are expected to be applicable. Under this circumstance, obtaining reliable statistics requires prohibitively large computing times, so that we have been forced to limit the numerical simulations to values of Reynolds numbers $R\leqslant R_c$.

The results are presented in Fig. 5, together with both the complete and the linearized solutions, Eqs. (69) and (70), respectively. The linear theory (Gaussian limit) shows quantitative agreement for values of R/R_c up to about 86%, but significant discrepancies start to show up as $R\to R_c$, where the theory leads to a diverging correlation function [cf. Eq. (70)]. This is not the case for the complete solution Eq. (69), which exhibits perfect quantitative agreement for R/R_c up to 95%. A relatively small discrepancy of about 8% is observed, however, for higher values of R. Although this discrepancy remains within the limit of the estimated statistical errors, its systematic aspect nevertheless requires some clarifications. In this respect, it is important to recall that the results derived in this section were valid up to $\mathcal{O}(u_0^2/c_s^2)$. Now, by definition $u_0/c_s=R\varepsilon$ [cf. Eq. (51)], and, since we have set $\varepsilon=10^{-2}$, $R_c\varepsilon\approx 0.13$ at the bifurcation point. This relatively large value of $R_c\varepsilon$ might well be at the origin of the observed discrepancy. To check the validity of this argument, it is tempting to perform the simulations all over again for a smaller value of ε. However, since the relaxation time

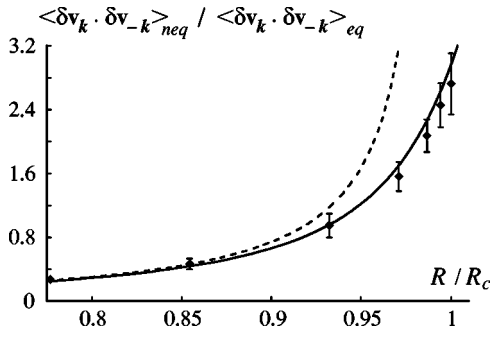

FIG. 5. Fourier transform of the nonequilibrium part of the static velocity autocorrelation function, normalized by the corresponding equilibrium part, as a function of R/R_c. The solid and dashed curves represent the complete and linearized solutions, Eqs. (69) and (70), respectively, whereas the diamonds correspond to numerical results obtained by the simulation of nonlinear compressible fluctuating hydrodynamic equations. The parameters are $a_r=2$, $\varepsilon=10^{-2}$, and $\mathcal{A}=10^{-3}/256$. The estimated statistical error is about 13% for the last data point.

of hydrodynamic modes grows as ε^{-1}, reaching the same degree of statistical accuracy as for the previous cases requires much longer running times. For this reason we decided to perform only one more simulation right at the critical point $R=R_c$, setting $\varepsilon=10^{-3}$. The theoretical prediction for the nonequilibrium part of the velocity correlation function is 2.31×10^{-6}. The simulation leads to 2.24×10^{-6} with an estimated statistical error of about 15%. The discrepancy is now about 3%, much better than for the case $\varepsilon=10^{-2}$.

IV. CONCLUDING REMARKS

Recently, we studied the statistical properties of linearized Kolmogorov flow, from near equilibrium up to the vicinity of the first instability leading to the formation of vortices [1]. In particular, we established that the incompressibility assumption leads to a wrong form of the static correlation functions, except near the instability threshold where numerical results suggest that the incompressibility assumption should remain valid. The clarification of this important issue requires a nonlinear analysis of fluctuating Kolmogorov flow. This is precisely the main purpose of the present article.

We first considered the case of an incompressible fluid. After identifying the slow modes governing the evolution of the system in the vicinity of the instability threshold, we performed an adiabatic elimination of the fast modes to obtain a set of two nonlinear Langevin equations for the slow modes. We then succeeded in deriving the explicit form of the stationary stream function, as well as the corresponding velocity profiles, in real space. Numerical studies of the nonlinear hydrodynamical equations allowed us to confirm our theoretical predictions.

We next considered the case of compressible Kolmogorov flow. The analysis can be simplified somewhat by noticing that the evolution of a compressible fluid is generally characterized by two different time scales: a slow one, related to the dissipative viscous modes, and a fast one, expressing the propagation of (damped) sound modes. The ratio of these time scales, denoted by ε [cf. Eq. 44)], can be considered as a small parameter, since otherwise the very validity of the hydrodynamics can no longer be guaranteed [32]. We thus have at our disposal a natural small parameter that can be used to set up a perturbative technique. As already mentioned, this method constitutes an alternative to the time scale perturbation theory that was generalized by Schmitz and Cohen in order to study the Bénard instability in a compressible fluid [15,33].

Using this perturbation technique, we first showed that the macroscopic behavior of the fluid is not affected, up to $\mathcal{O}(u_0^2/c_s^2)$, by the compressibility, in agreement with the intuitive arguments presented in the Introduction. We then succeeded in establishing that, close to the instability threshold, the stochastic dynamics of the system is governed by two coupled nonlinear Langevin equations in Fourier space. The solution of these equations can be cast into the exponential of a Landau-Ginzburg functional which, to dominant order in ε, proves to be identical to the one obtained for the case of the incompressible fluid. The theoretical predictions were confirmed by numerical simulations of the nonlinear fluctuating hydrodynamic equations.

ACKNOWLEDGMENTS

We are very grateful to Professor E. G. D. Cohen, Professor G. Nicolis, Professor J. W. Turner, and Professor C. Van den Broeck for helpful comments. This work was supported by the Belgian Federal Office for Scientific, Technical and Cultural Affairs within the framework of the ''Pôles d'attractions interuniversitaires'' program, and by a European Commission DG 12 Grant No. PSS*1045.

[1] I. Bena, M. Malek Mansour, and F. Baras, Phys. Rev. E **59**, 5503 (1999).
[2] L. D. Landau and E. M. Lifshitz, *Fluid Mechanics* (Pergamon, Oxford, 1984).
[3] T. R. Kirkpatrick, E. G. D. Cohen, and J. R. Dorfman, Phys. Rev. Lett. **42**, 862 (1979); **44**, 472 (1980); Phys. Rev. A **26**, 995 (1982).
[4] J. Dufty, in *Spectral Line Shapes*, edited by P. Wende (De Kruger, Berlin, 1981); J. Lutsko and J. Dufty, Phys. Rev. A **32**, 1229 (1985).
[5] I. Procaccia, D. Ronis, and I. Oppenheim, Phys. Rev. Lett. **42**, 287 (1979); D. Ronis, I. Procaccia, and I. Oppenheim, Phys. Rev. A **19**, 1324 (1979); A. -M. Tremblay, M. Arai, and E. Siggia, *ibid.* **23**, 1451 (1981); D. Ronis, I. Procaccia, and I. Oppenheim, *ibid.* **26**, 1812 (1982).
[6] G. Van der Zwan, D. Bedeaux, and P. Mazur, Physica A **107**, 491 (1981); R. Schmitz and E. G. D. Cohen, J. Stat. Phys. **39**, 285 (1985); **40**, 431 (1985).
[7] J. Machta, I. Procaccia, and I. Oppenheim, Phys. Rev. Lett. **42**, 1368 (1979); J. Machta, I. Oppenheim, and I. Procaccia, Phys. Rev. A **22**, 2809 (1980).
[8] R. Schmitz, Phys. Rep. **171**, 1 (1988).
[9] B. M. Law and J. V. Sengers, J. Stat. Phys. **57**, 531 (1989); B.

M. Law, P. N. Segré, R. W. Gammon, and J. V. Sengers, Phys. Rev. A **41**, 816 (1990).
[10] M. Malek Mansour, A. L. Garcia, G. Lie, and E. Clementi, Phys. Rev. Lett. **58**, 874 (1987); M. Mareschal, M. Malek Mansour, G. Sonino, and E. Kestemont, Phys. Rev. A **45**, 7180 (1992).
[11] A. Suárez, J. P. Boon, and P. Grosfils, Phys. Rev. E **54**, 1208 (1996).
[12] A. L. Garcia, M. Malek Mansour, G. Lie, M. Mareschal, and E. Clementi, Phys. Rev. A **36**, 4348 (1987).
[13] V. M. Zaitsev and M. I. Shliomis, Zh. Éksp. Teor. Fiz. **59**, 1583 (1970) [Sov. Phys. JETP **32**, 866 (1971)].
[14] R. Graham, Phys. Rev. A **10**, 1762 (1974); R. Graham and H. Pleiner, Phys. Fluids, **18**, 130 (1975); J. Swift and P. C. Hohenberg, Phys. Rev. A **15**, 319 (1977).
[15] R. Schmitz and E. G. D. Cohen, J. Stat. Phys. **39**, 285 (1985); **40**, 431 (1985).
[16] A. M. Obukhov, Russ. Math. Survey **38**, 113 (1983).
[17] S. Gama, M. Vergassola, and U. Frisch, J. Fluid Mech. **260**, 95 (1994).
[18] E. N. Lorenz, J. Fluid Mech. **55**, 545 (1972).
[19] Z. S. She, Phys. Lett. A **124**, 161 (1987); Ph.D. thesis, University of Paris VII, 1987 (unpublished); G. I. Sivashinsky, Physica D **17**, 243 (1985).
[20] R. Benzi and S. Succi, J. Stat. Phys. **56**, 69 (1989); U. Frisch, B. Legras, and B. Villone, Physica D **94**, 36 (1996).
[21] L. Meshalkin and Ya. G. Sinai, J. Appl. Math. Mech. **25**, 1140 (1961).
[22] J. S. A. Green, J. Fluid Mech. **62**, 273 (1974).
[23] This result is not new and has been obtained by several authors, like, for instance, A. A. Nepomniaschichii, J. Appl. Math. Mech. **40**, 836 (1976); [21]; [18].
[24] C. Machioro, Commun. Math. Phys. **105**, 99 (1986).
[25] H. Haken, *Synergetics, An Introduction*, 3rd ed., Vol. 1 of *Springer Series in Synergetics* (Springer, Berlin, 1983).
[26] G. Nicolis, *Introduction to Nonlinear Science* (Cambridge University Press, Cambridge, 1995).
[27] F. Baras, M. Malek Mansour, and C. Van Den Broeck, J. Stat. Phys. **28**, 577 (1982).
[28] G. M. Zaslavsky, R. Z. Sagdeev, D. A. Usikov, and A. A. Chernikov, *Weak Chaos and Quasi-Regular Patterns* (Cambridge University Press, Cambridge, England, 1991), Chap. 9.
[29] C.-Y. Chow, *An Introduction to Computational Fluid Mechanics* (Seminole Publ., Boulder, CO, 1983).
[30] This result has already been obtained by M. A. Brutyan and P.L. Krapivsky, Eur. J. Mech. Fluids B **11**, 587 (1992) for a compressible fluid in the limit of infinite aspect ratio.
[31] C. Van den Broeck, M. Malek Mansour, and F. Baras, J. Stat. Phys. **28**, 557 (1982).
[32] See, for instance, W. E. Alley and B. J. Alder, Phys. Rev. A **27**, 3158 (1983); W. E. Alley, B. J. Alder, and S. Yip, *ibid.* **27**, 3174 (1983).
[33] U. Geigenmüller, U. M. Titulaer, and B. U. Felderhof, Physica A **119**, 41 (1983).